Composition Dependence of the Nucleation Energy of Iron Antimonides from Modulated Elemental Reactants

Joshua R. Williams, Mark Johnson, and David C. Johnson*

Contribution from the Department of Chemistry and Materials Science Institute, University of Oregon, Eugene, Oregon 97403

Received October 26, 2000

Abstract: Modulated elemental reactants containing iron and antimony were found to react at low temperature (T < 200 °C) forming either $FeSb_2$ or $FeSb_3$ depending on both the layer thicknesses and the overall composition of the initial reactant. For films containing 75% antimony and 25% iron, the metastable compound $FeSb_3$ was observed to nucleate and grow if the layer thickness was below approximately 35 Å. Above this critical thickness for the modulation, annealing led to the formation of $FeSb_2$. This, combined with low-angle diffraction data, suggests that the initial interdiffusion between iron and antimony layers in an elementally modulated reactant results in the formation of an amorphous reaction intermediate if the layering thickness is less than 35 Å. For modulated reactants with composition between 70 and 90 atomic % antimony and below this critical layer thickness, the metastable compound $FeSb_3$ formed. In more iron-rich modulated reactants $FeSb_2$ nucleates. The nucleation temperature and the nucleation energy of $FeSb_3$ were found to be a function of the composition of the amorphous intermediate, while those of $FeSb_2$ were found to be relatively independent of composition.

Introduction

Every organic chemist knows that knowledge of reaction mechanisms is critical to controlled synthesis. A reaction mechanism provides guidance for optimizing yields as well as extending a reaction to new reactants. Relative to molecular chemistry, the situation in solid-state chemistry is complicated because the reacting systems are generally heterogeneous, temperatures are usually quite high, and techniques to follow reactions are very limited. Despite these difficulties, there has been increasing emphasis by solid-state chemists aimed at understanding the kinetics and mechanism of solid-state reactions because there are undoubtedly a great number of very interesting compounds that would be kinetically stable if we only knew how to make them.[1,2]

Our approach to this challenge has been the development of modulated elemental reactants. In this approach, we use high-vacuum deposition techniques to deposit alternating layers of desired elements. This approach gives angstrom level control of the thickness of each layer, allowing the diffusion distances and composition within each reactant to be controlled. We have shown that with this approach we have the ability to prepare metastable compounds if these compounds nucleate before the competing thermodynamically more stable phases in the relevant phase diagrams. The designed nature of the starting reactant also permits us to explore the reaction mechanism as a function of the structure of the initial reactant.[3]

Recently we were able to prepare the metastable compound $FeSb_3$ with the skutterudite structure type.[4] This structure type has been shown to be potentially useful as a thermoelectric. Thermoelectrics are materials that create a temperature differential when a current is passed through them. The compound $CoSb_3$ with the skutterudite structure has been shown to have a large Seebeck coefficient (the voltage produced by a temperature differential across a sample) and a low resistivity, both of which are important for thermoelectric devices.[5] What makes this structure type potentially very useful as a thermoelectric, however, is that skutterudites have been shown to be a member of a class of materials that behave as glasses with respect to thermal transport but as crystals with respect to their electron transport properties.[6] This phonon glass-electron crystal behavior, first proposed by Slack,[7] results from the large amplitude of vibration of a ternary cation, M′, in the $M'_xM_4Sb_{12}$ filled skutterudite structure. The M′ cation resides in a 12-coordinate site in the crystal and the size of this site is determined by the atomic radius of the antimony.[8] The amplitude and frequency of the vibration depends on the size and mass of the ternary M′ cation, with small, heavy cations scattering lower frequency lattice vibrations. Compounds with small and heavy M′ atoms on one crystallographic site are desired to lower thermal conductivity while substitutions on the other sites optimize the electrical properties by controlling the number of carriers. Unfortunately, many compounds of this type, for example $Lu_yCo_xFe_{4-x}Sb_{12}$, are thermodynamically unstable for all x and y presumably because of the weak bonding of the small M′ cation.[9]

(1) Brewer, L. *J. Chem. Educ*. **1958**, *35*, 153.
(2) Stein, A.; Keller, S. W.; Mallouk, T. E. *Science* **1993**, *259*, 1558−1564.
(3) Johnson, D. C. *Curr. Opin. Solid State Mater. Sci.* **1998**, *3*, 159−167.
(4) Hornbostel, M. D.; Hyer, E. J.; Thiel, J. P.; Johnson, D. C. *J. Am. Chem. Soc.* **1997**, *119*, 2665−2668.
(5) Caillat, T.; Borshchevsky, A.; Fleurial, J. P. *J. Appl. Phys.* **1996**, *80*, 4442−4449.
(6) Sales, B. C.; Mandrus, D.; Williams, R. K. *Science* **1996**, *272*, 1325−1328.
(7) Rowe, D. M. *CRC Handbook of Thermoelectrics*; Eds. CRC Press: Boca Raton, FL, 1995; pp 407−440.
(8) Braun, D. J.; Jeitschko, W. *J. Less-Common Met.* **1980**, *72*, 147−156.
(9) Nolas, G. S.; Slack, G. A.; Morelli, D. T.; Tritt, T. M.; Ehrlich, A. C. *J. Appl. Phys*. **1996**, *79*, 4002−4008.

10.1021/ja003791d CCC: $20.00
Published on Web 02/02/2001

The interest in skutterudites as thermoelectric materials has resulted in significant synthesis activity aimed at preparing new members of this structure type. The original structure of skutterudite was determined from a naturally occurring crystal of $CoAs_3$ first found in Skutterud, Norway. The corresponding binary compounds MX_3, where M = Co, Rh, Ir and X = P, As, and Sb, along with the isostructural nickel compound NiP_3, have all been shown to be thermodynamically stable compounds at atmospheric pressure and below the temperatures at which they peritectically decompose.[5] As mentioned earlier, ternary "filled skutterudite" compounds have also been prepared.[8] In the ternary phosphorus and arsenic skutterudites, the occupancy of the ternary cation site in $M'_xM_4X_{12}$, x, ranges from 0 to 1. For the ternary antimonides $M'_xCo_4Sb_{12}$, however, M′ must be a large electropositive cation and only partial occupancy (less than 25%) is possible via traditional synthesis techniques.[9,10] Some ternary compounds MFe_4Sb_{12} are thermodynamically stable at atmospheric pressure and below temperatures at which they peritectically decompose, but only for large M atoms such as Ba, La, and some of the early rare earths.[8,11] The binary compound $FeSb_3$ and ternary compounds MFe_4Sb_{12}, where M is a small cation such as a later rare earth metal or a post transition metal such as indium, tin, or lead, are not thermodynamically stable.[12]

The ability to prepare the metastable compounds $FeSb_3$ and ternary skutterudites with small ternary cations from modulated elemental reactants at low temperatures (less than 200 °C) prompted us to explore the reaction mechanism of skutterudite formation. This paper explores the effect of both layer thickness and composition on the evolution of Fe−Sb modulated reactants. A critical thickness for the repeating unit of the modulated reactant is observed, below which the metastable binary compound $FeSb_3$ forms if the composition is greater than 75 atomic % antimony. If the repeat thickness is greater or if the composition is more iron rich, the thermodynamically stable compound $FeSb_2$ is formed. We have measured the nucleation temperature and the activation energy for nucleation as a function of composition. These results provide insight for a rational strategy for the synthesis of other metastable compounds.

Experimental Section

The elementally modulated reactants were prepared in a high-vacuum evaporation system that has been described in detail elsewhere. Briefly, the elements were sequentially deposited in high vacuum (lower than. 5×10^{-7} Torr) under the control of a personal computer. The pumping of the deposition system is by a CTI cryopump. The gas pressure during deposition was limited by the outgassing of the deposition sources but was typically below 1×10^{-7} Torr. Iron was deposited from electron beam evaporation sources at a rate of 0.5 Å/s. Antimony was deposited using an effusion cell at approximately the same rate. Each deposition source was independently monitored using a quartz crystal thickness monitor allowing the thickness of each elemental layer to be controlled to better than the nearest angstrom. The repeat thickness (sum of the individual elemental thicknesses) for all of the samples was varied to determine the critical thickness at which the system did not interfacially nucleate. All subsequent films were prepared with a total layer thickness well below this critical thickness (35 Å) to increase the probability that the films would interdiffuse at low temperatures without nucleating binary compounds at the reacting interfaces. The elemental composition of the samples was found to be repeatable to within about 5% over a period of several months. The films were simultaneously deposited on silicon chips and photoresist-coated silicon wafers. The silicon substrates were used for low-angle diffraction studies. Free-standing films were prepared from the coated substrates by soaking them in acetone, which dissolved the photoresist. The elementally modulated film particles were collected from the acetone by filtration with Teflon filters. These free-standing films were used in the calorimetry investigations.

Table 1. Summary of Samples Prepared To Determine Critical Thickness

sample	Fe intend	Sb intend	intended	actual	A % Sb	A % Fe	phase
A-4	1.4	29.4	30.8	26	78.2	21.8	$FeSb_3$
A-3	2.2	44.1	46.3	44	84.9	15.1	$FeSb_2$
A-2	2.9	58.8	61.8	53	85.2	14.8	$FeSb_2$
A-1	3.7	73.5	77.2	80	84.6	15.4	$FeSb_2$

Low-angle X-ray diffraction was used to characterize the multilayer periodicity and to study the interdiffusion of the elements. The repeat thickness was determined from the position of the Bragg diffraction maxima. The total film thickness was determined from the higher frequency oscillations resulting from interference of the X-rays between the front and back of the films. High-angle X-ray diffraction was used to identify crystalline compounds. Copper Kα radiation was used in both the low- and high-angle diffraction studies that were performed on a Scintag XDS 2000 diffractometer. The average composition of the multilayer films was determined by electron microprobe analysis using an energy-dispersive X-ray detector.

Samples were annealed in a nitrogen atmosphere or in a dynamic vacuum better than 10^{-5} Torr. Substrate-free samples were annealed in a differential scanning calorimeter cell under flowing nitrogen. Measured exotherms were correlated with X-ray results to identify and track the interdiffusion of the elements and the crystallization of any compounds.

Results

We prepared over 35 samples containing repeating thin elemental layers of iron and antimony to explore the effect of both layer thickness and composition on the kinetics of phase formation. The samples contained in Table 1 were prepared to determine the effect of layer thickness on the evolution of the initial reactants. The samples in Table 2 were all prepared with layer thicknesses below the critical layer thickness determined from the samples in Table 1. The samples with labels starting with the letter B in Table 2 were all prepared with a constant antimony layer thickness of 11.3 Å. The iron layer thickness was then varied systematically to change the overall composition. The samples with labels starting with the letter C were all prepared with a constant iron layer thickness of 0.3 Å. Figure 1 illustrates the agreement between the intended total repeat layer thickness and that measured using low-angle X-ray diffraction. In all cases the agreement is within 2 Å. The actual thickness was determined using either Bragg diffraction maxima or the higher frequency maxima resulting from interference between X-rays reflected from the sample surface and the silicon−sample interface. Compositions determined from microprobe analysis agree well with that calculated from the intended layer thicknesses using reasonable estimates for the density of the deposited elements.

We prepared the samples in Table 1 to investigate the effect of layer thickness on phase formation at the reacting iron−antimony interface. All of the samples in Table 1 have similar compositions, containing approximately 80% antimony and 20% iron. Bulk reaction of iron and antimony results in the formation of sequential layers of the known binary compounds as layers on the surface of the iron particles. This is expected, as binary diffusion couples have long been a powerful tool for the

(10) Meisner, G. P.; Morelli, D. T.; Hu, S.; Ynag, Y.; Uher, C. *Phys. Rev. Lett.* **1998**, *80*, 3551−3554.
(11) Evers, C. B. H.; Jeitschko, W.; Boonk, L.; Braun, D. J.; Ebel, T.; Scholz, U. D. *J. Alloys Compd.* **1995**, *224*, 184−189.
(12) Sellinschegg, H.; Stuckmeyer, S. L.; Hornbostel, M. D.; Johnson, D. C. *Chem. Mater.* **1998**, *10*, 1096−1101.

Table 2. Summary of Samples Prepared To Determine the Composition Dependence of the Nucleation Energy

sample	Fe intend	Sb intend	intended	actual	A % Sb	A % Fe	phase	N.E.
B-1	1.2	14.7	15.9	15	77.7	22.3	$FeSb_3$	2.143
B-2	0.7	11.3	12.0	12	79.0	21.0	$FeSb_3$	1.618
B-3	0.9	11.3	12.1	11	81.6	18.4	$FeSb_3$	1.444
B-4	0.5	11.3	11.8	11	86.2	13.8	$FeSb_3$	1.659
B-5	0.6	11.3	11.9	11	82.6	17.4	$FeSb_3$	1.470
B-6	0.8	11.3	12.0	11	75.5	24.5	$FeSb_3$	1.905
B-7	1.0	11.3	12.2	11	71.1	28.9	$FeSb_2$	1.401
B-8	1.0	11.3	12.3	13	71.0	29.0	$FeSb_2$	1.540
B-9	1.1	11.3	12.4	12	68.7	31.3	$FeSb_2$	1.375
B-10	1.2	11.3	12.5	66.3	33.7	$FeSb_2$	1.532	
B-11	1.3	11.3	12.6	12	65.7	34.3	$FeSb_2$	1.511
B-12	1.4	11.3	12.6	12	38.1	61.9	$FeSb_2$	1.462
B-13	1.5	11.3	12.7	12	66.3	33.7	$FeSb_2$	1.599
B-14	1.6	11.3	12.9	12	76.7	23.3	$FeSb_3$	1.528
B-15	1.6	11.3	12.9	12	76.7	23.3	$FeSb_2$	1.344
B-16	1.6	11.3	12.8	61.7	38.3	$FeSb_2$	1.542	
B-17	0.4	11.3	11.7	11	85.2	14.8	$FeSb_3$	1.662
B-18	0.3	11.3	11.6	10	80.2	19.8	$FeSb_3$	1.634
B-19	1.0	11.3	12.2	12	81.5	18.5	$FeSb_3$	1.504
B-20	1.5	11.3	12.7	12	75.7	24.3	$FeSb_3$	1.578
B-21	1.5	11.3	12.7	12	75.7	24.3	$FeSb_2$	1.532
C-1	0.3	10.4	10.7	10	67.8	32.2	$FeSb_2$	
C-2	0.3	9.5	9.9	9	68.3	31.7	$FeSb_2$	
C-3	0.3	8.7	9.0	9	69.4	30.6	$FeSb_2$	1.570
C-4	0.3	12.1	12.5	13	76.6	23.4	$FeSb_3$	1.698
C-5	0.3	13.0	13.3	13	77.2	22.8	$FeSb_3$	1.513
C-6	0.3	13.9	14.2	14	83.4	16.6	$FeSb_3$	
C-7	0.3	7.8	8.1	7	74.5	25.5	$FeSb_3$	1.604
C-8	0.3	6.9	7.3	8	75.1	24.9	$FeSb_2$	1.487
C-9	0.3	6.1	6.4	8	77.1	22.9	$FeSb_3$	1.422
C-10	0.3	7.8	8.1	8	83.0	17.0	$FeSb_3$	1.606
C-11	0.3	5.2	5.5	5	77.8	22.2	$FeSb_3$	1.685
C-12	0.3	11.3	11.6	11	85.9	14.1	$FeSb_3$	1.654
C-13	0.3	4.3	4.7	5	69.4	30.6	$FeSb_2$	1.470
C-14	0.3	12.1	12.5	12	86.0	14.0	$FeSb_3$	1.788

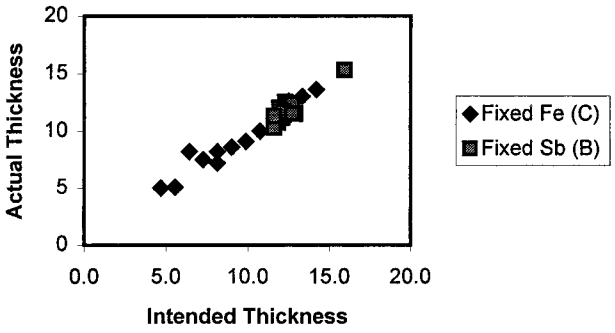

Figure 1. Actual measured layer thickness vs intended layer thickness.

investigation of phase diagrams.[13] As annealing time or annealing temperature increases, the thickness of the binary compounds increases. Sample A-1, which contains the thickest elemental bilayers we prepared, shows this behavior. Figure 2 contains the DSC of this reactant and Figures 3 and 4 contain the low- and high-angle X-ray diffraction patterns, respectively. The DSC data contain a sharp exotherm at 200 °C resulting from the nucleation of $FeSb_2$. The as-deposited low-angle diffraction pattern shows Bragg diffraction maxima resulting from the elemental layering in the sample while the sample is amorphous to high-angle diffraction. Annealing the sample above 200 °C results in the formation of crystalline $FeSb_2$ as seen in the high-angle diffraction pattern. The low-angle diffraction pattern still contains Bragg diffraction maxima after

(13) Brophy, J. H.; Rose, R. M.; Wulff, J. *The Structure and Properties of Materials*; Wiley: New York, 1964; Vol. 2.

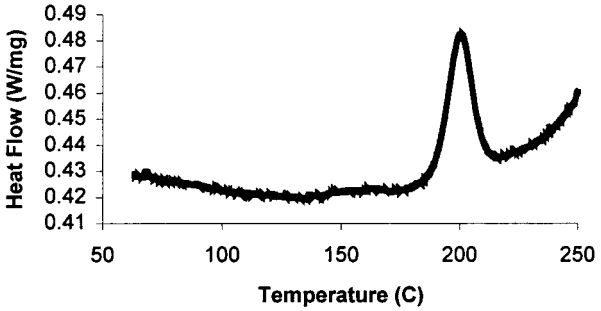

Figure 2. DSC of A-1 showing a large exotherm at 200 °C.

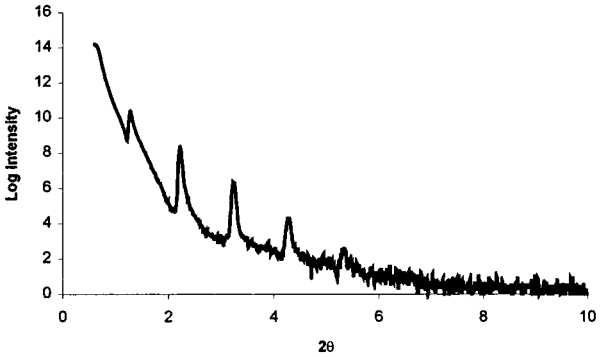

Figure 3. Low-angle X-ray diffraction patterns of A-1 before and after annealing.

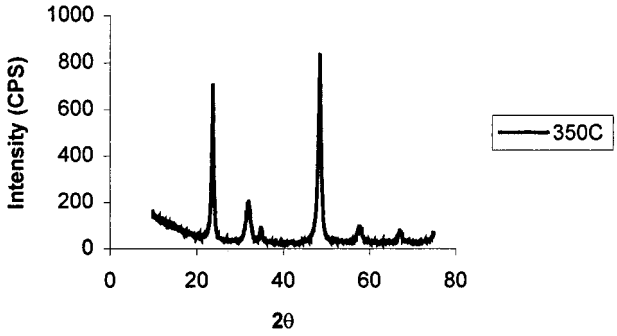

Figure 4. High-angle X-ray diffraction patterns of A-1 before and after annealing.

annealing, indicating that at least part of the sample is still compositionally modulated. These data suggest that crystalline $FeSb_2$ formed at the reacting interfaces in a manner similar to that observed in bulk diffusion couples.

The thinnest sample listed in Table 1 reacted much differently. The DSC data obtained on this sample look very similar to that shown in Figure 2, except with the exotherm at 134 °C, and the corresponding high- and low-angle X-ray diffraction data are shown in Figures 5 and 6. This thin sample remains amorphous while the layers interdiffuse at temperatures below the large exotherm at 134 °C in the DSC. After the exotherm, the high-angle diffraction pattern is that of a cubic material. Reitveld refinement of this pattern indicates that the sample has formed a crystalline skutterudite structure with composition $FeSb_3$.

Figure 7 is a representation of what we believe is occurring in these samples as a function of annealing. The first reaction step in both of the samples is interdiffusion of iron and antimony. In the thin sample the composition gradients differ from those in the thick sample because of the limited supply of both of the elements. When the diffusion distance is short, as in the thin-layered samples, the elements completely interdiffuse before nucleation can occur. The amorphous intermediate that

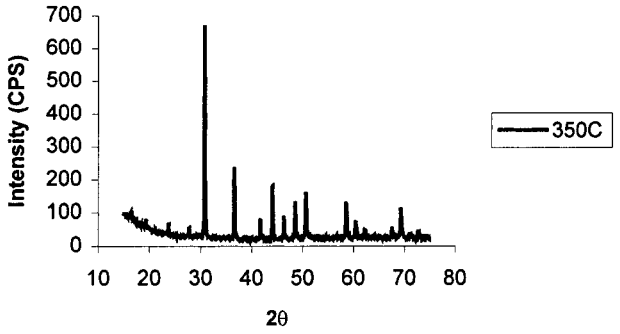

Figure 5. High-angle X-ray diffraction patterns of A-4 before and after annealing.

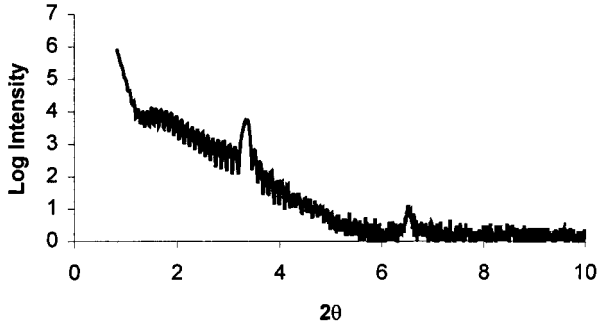

Figure 6. Low-angle X-ray diffraction patterns of A-4 before and after annealing.

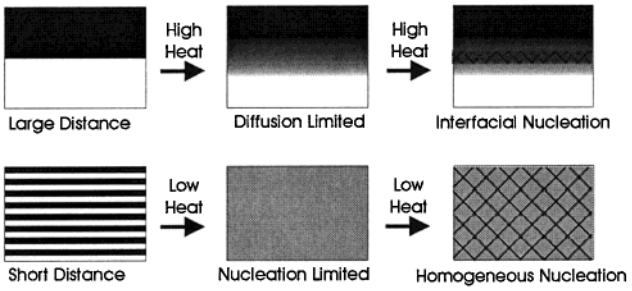

Figure 7. Cartoon depicting one possible explanation for the diffusion and nucleation processes in this system.

results has the composition of the original multilayered elemental reactant. Consequently, when sufficient energy is available to form $FeSb_2$, there is no region of the sample with this composition, preventing its nucleation. The metastable compound $FeSb_3$ crystallizes instead of $FeSb_2$, as it is the easier compound to nucleate from the amorphous composition. In the thicker samples, however, there is a nearly complete composition gradient between Fe and Sb, leading to the nucleation of $FeSb_2$ at the appropriate composition as the temperature is raised. Thus there exists a critical thickness for the reacting multilayered samples. If the samples are above this critical thickness, the thermodynamically expected compounds nucleate and grow at the reacting interfaces. If the samples are thinner than this critical thickness, the diffusion distance is short enough that the samples interdiffuse significantly before nucleating. This limits the range of compositions at the reacting interface, preventing, in this case, the nucleation of $FeSb_2$. Low reaction temperatures are important, as the low diffusion rates of the elements in the amorphous solid at low temperatures prevents the disproportionation of the sample into the expected thermodynamically stable compounds. This provides time for the nuclei of the metastable compound $FeSb_3$ to form.

To test this hypothesis and to determine the effect of composition on the formation of $FeSb_3$, we prepared the samples

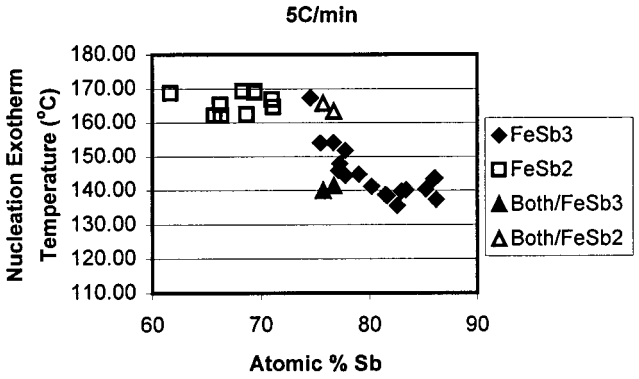

Figure 8. The nucleation exotherm temperature clearly depends on the composition of the sample.

contained in Table 2. All of these samples were prepared with repeat layer thicknesses well below the critical thickness determined by using the samples in Table 1. As was done for the samples in Table 1, we measured the heat flow as a function of temperature by using DSC and used X-ray diffraction to follow the structural evolution of each of these samples. We show in Figure 8 the nucleation exotherm temperature as a function of sample composition. This clearly shows the difference in nucleation temperature between the two phases, and also shows that the nucleation temperature for samples that formed $FeSb_3$ appears to depend more strongly on composition than for those samples that formed $FeSb_2$.

To determine the kinetic stability of the reaction intermediate present before the exotherm, we collected differential scanning calorimetry data as a function of scan rate to estimate the activation energy of the nucleation and growth process. We analyzed this nonisothermal DSC data using the method described by Kissinger[14] in which the activation energy can be obtained from the shift in peak temperature, T_p, as a function of scan rate, Q:

$$\frac{\mathrm{d}\ln[Q/T_p^2]}{\mathrm{d}[1T_p]} = \frac{-E_{\mathrm{crystallization}}}{R}$$

This equation is derived by assuming that the nucleation and growth can be described by the Johnson−Mehl−Avrami equation, that the initial and the final states have the same composition, and that the nucleation and growth rates are constant at constant temperature. A further approximation is made that both the nucleation rate and growth rates may be described by Arrhenius expressions over the range of temperature in which the peak temperature varies with scan rate. Graphing $\ln Q/T_p^2$ versus $1/T_p$ gives a straight line with slope $-E/R$. Figure 9 contains a plot of the activation energies obtained using this method of analysis as a function of composition. The squares (■ or □) indicate samples created with constant Sb layer thickness. The circles (● or ○) indicate samples created with a constant Fe layer thickness. The diamonds (▲ or △) indicate samples that were made with a constant Sb layer thickness but nucleated both binary compounds. Samples containing more than 25% iron were observed to form $FeSb_2$ with activation energy near 1.5 eV without any strong dependence on composition. Samples containing less than 20% iron were observed to form $FeSb_3$ with activation energies ranging from 1.42 to 2.14 eV with the higher nucleation energies occurring near the extremes in the observed composition range in which this compound formed. Two samples close to 25%

(14) Kissinger, H. E. *Anal. Chem.* **1957**, *29*, 1702−1706.

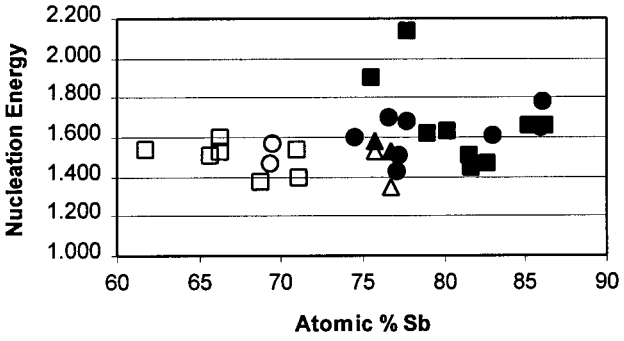

Figure 9. A plot of the measured nucleation energy versus composition. The unfilled markers are samples that nucleated $FeSb_2$ and the filled markers are samples that nucleated $FeSb_3$.

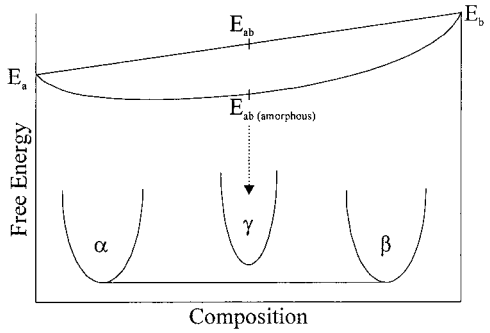

Figure 10. A general view of the reaction processes involved in the synthesis described in this paper.

iron in composition were observed to nucleate both compounds. In these cases, $FeSb_3$ nucleated first followed by the formation of $FeSb_2$. While there is no clear composition dependence to the nucleation energy for either compound, the composition of the amorphous intermediate is crucial in determining which compound nucleates.

A general view of the diffusion and nucleation processes proposed for samples with repeat layer thickness below the critical layer thickness is shown pictorially in Figure 10. The energy of a binary modulated elemental reactant will approximately be that of a heterogeneous mixture of the two constituent materials (labeled E_{ab}). Raising the temperature permits the system to interdiffuse, lowering the free energy of the system by the heat of mixing. If this can be accomplished at relatively low temperatures, the resulting mixture will be amorphous. At low temperatures, there is not enough energy to nucleate a crystalline compound. On raising the temperature, the metastable phase γ should nucleate because the composition of the mixture is much closer to that of the phase γ than either of the thermodynamically stable phases α or β. The low diffusion rate in the amorphous intermediate at these temperatures prevents the disproportionation of the sample via long-range diffusion into the thermodynamically stable compounds. The low diffusion rate prevents the assembly of a nucleus which deviates significantly from the average composition. This is functionally similar to the use of blocking groups in organic synthesis, which prevent the close approach of a reactant to a reactive site in a molecule. In both cases, access to a reaction intermediate is prevented through manipulating diffusion rates. These same principles could be applied to ternary and higher order systems where the presence of a third material in the mixture (that cannot be incorporated into a binary compound) could inhibit the formation of more stable binary compounds over a broad composition range. This potentially will allow access to ternary and higher order compounds that are thermodynamically unstable (but kinetically stable) with respect to the known binary compounds.

Summary

It has been shown that the reaction of thin layers of Fe and Sb to form either $FeSb_2$ or $FeSb_3$ is dependent on layer thickness and composition. If the layer thickness is below approximately 35A, and the composition is at least 75 atomic % Sb, $FeSb_3$ nucleates. If either the composition is less than 75 atomic % Sb or the layer thickness is above 35A, $FeSb_2$ nucleates. Low-angle X-ray diffraction data show that this thickness dependence results from incomplete diffusion for thick-layered samples. Heterogeneous nucleation occurs before diffusion is complete. By contrast, thin-layered samples appear to diffuse completely and form an amorphous intermediate, which then undergoes homogeneous nucleation. Although there is an abrupt change in the phase that nucleates as a function of composition, the nucleation energy of samples that nucleated $FeSb_2$ and $FeSb_3$ were both shown to be relatively independent of composition.

JA003791D